Shell-correction method for calculating the binding energy of metal clusters: Application to multiply charged anions

C. Yannouleas and Uzi Landman
School of Physics, Georgia Institute of Technology, Atlanta, Georgia 30332-0430
(Received 3 February 1993)

Utilizing the nuclear-physics concept of separating, as a function of size, the total energy of a finite system into two parts, a *smooth* contribution and a shell correction, we introduce a method of calculating the binding energy of metal clusters. The method consists of a determination of the smooth part of the total energy from an extended Thomas Fermi approach to density-functional theory, and of superimposing on it a shell correction introduced through the kinetic-energy contribution. While circumventing a self-consistent iterative solution of the effective single-particle Kohn-Sham equations, the present method yields results in excellent agreement with such self-consistent calculations, but with considerable savings in computation time, thus allowing for an efficient approach for accurate systematic investigations of cluster properties for a wide range of sizes. As an application of the method, we study energetics and decay modes of multiply charged anionic metal clusters. Singly charged anions are stable for all sizes, but multiply charged negative ions are stable against spontaneous electron decay only above certain critical sizes. Below the border of stability, the cluster anions are metastable against electron tunneling through a Coulombic barrier. Lifetimes for such decay processes are estimated. Fission channels, which may compete with electron autodetachment, are studied for the case of doubly charged anions.

I. INTRODUCTION

Numerous observations pertaining to the size dependence of physical and chemical properties of material clusters provide the impetus for investigations aiming at the elucidation of the physical origins, nature, and systematics of size-evolutionary patterns (SEP's) of the properties of clusters as their degree of aggregation varies from the atomic and molecular scale to the condensed-phase regime.[1]

Outstanding examples of SEP's are provided by simple metal clusters, where experimental and theoretical investigations have unveiled the importance of an electronic shell structure for providing a unified framework for the analysis of size-dependent trends of energetics, stability, spectral characteristics, and fragmentation patterns in these systems.[2,3] Moreover, several properties of such elemental clusters (e.g., shell structure, and most recently supershells,[4] portrayed by the occurence of magic numbers in the abundance spectra and ionization potentials;[2] giant spectral resonances interpreted as evidence for collective plasma oscillations;[5–7] and barrier shapes,[8] fragmentation, and fission patterns of ionized clusters[8–11]) bear close analogies to the corresponding phenomena exhibited by atomic nuclei.[12,13]

These analogies have led to the adaptation of several concepts and methodologies developed in the context of nuclear-physics phenomena for the interpretation of recent studies of elemental clusters.[4,7,14–16] In particular, experimental results pertaining to fragmentation patterns (symmetric versus asymmetric fission) and fission barriers have been interpreted using the framework of the celebrated liquid-drop model (LDM) of nuclear fission,[12] and predictions of energetics and fission channels were made using the jellium model[11] (we note that while a limited number of calculations, up to 40 atoms, for the ground-state properties of Na and Cu clusters have been performed for axially deformed (spheroidal) jellium droplets,[17,18] most self-consistent calculations for jellium droplets are restricted to spherical symmetry[11,19,20]). In this context, we mention other theoretical investigations which preserve the particulate nature of elemental clusters, and thus are applicable to general cluster geometries, based on quantum-chemical techniques[21] or density-functional theory (DFT) in conjunction with pseudopotentials.[8,22] These methods, which provide important structural, energetic, spectral, and dynamic information, involve significant computational efforts, and usually have been applied to rather small systems.

It has long been recognized in nuclear physics that the dependence of ground-state properties of nuclei on the number of particles can be viewed as the sum of two contributions: the first contribution varies smoothly with the particle number (number of protons N_p and neutrons N_n) and is referred to as the *smooth* part; the second contribution gives a superimposed structure on the smooth curve and exhibits an oscillatory behavior, with extrema at the nuclear magic numbers.[12,13]

Nuclear masses have provided a prototype for this behavior.[12] Indeed, the main contributions to the exper-

0163-1829/93/48(11)/8376(12)/$06.00

imental nuclear binding energies are smooth functions of the number of protons and neutrons, and are described by the semiempirical mass formula.[23,24] The presence of these smooth terms led to the introduction of the LDM, according to which the nucleus is viewed as a drop of a nonviscous fluid whose total energy is specified by volume, surface, and curvature contributions.[12,25,26]

The deviations of the binding energies from the smooth variation implied by the LDM have been shown[26–29] to arise from the shell structure associated with the bunching of the discrete single-particle spectra of the nucleons, and are commonly referred to as the shell correction.[30] Substantial progress in our understanding of the stability of strongly deformed open-shell nuclei and of the dynamics of nuclear fission was achieved when Strutinsky proposed[27,28] a physically motivated efficient way of calculating the shell corrections. The method consists of averaging (see below) the single-particle spectra of phenomenological deformed potentials and of subtracting the ensuing average from the total sum of single-particle energies.

Later it was realized that the self-consistent Hartree-Fock ground-state energies (the Hartree-Fock approach expresses the mean-field picture of the nucleus), can be separated[29,31] into a smooth contribution and a shell-correction part, in analogy with the known behavior of the empirical masses. More importantly, it was shown[31,32] that the smooth contribution extracted from the nuclear Hartree-Fock potentials according to Strutinsky's averaging method can be determined accurately by using a variationally optimized density resulting from a semiclassical extended Thomas-Fermi (ETF) approach to density-functional theory. The full oscillatory behavior of the self-consistent Hartree-Fock energies is recovered by adding Strutinsky's shell correction.

While certain analogies, portrayed in experimental data, between properties of nuclei and elemental clusters have been recognized, as mentioned above, the nuclear-physics approach of separating the various quantities as a function of size into a smooth part and a shell-correction part has only partially been explored in the case of metal clusters. In particular, several investigations[33–36] used the ETF method in conjunction with the jellium approximation to determine the average (smooth, in the sense defined above) behavior of metal clusters, but have not pursued a method for calculating the shell corrections.

In the absence of a method for appropriately calculating shell corrections for metal clusters in the context of the semiclassical ETF method, it has been presumed that the ETF method is most useful for larger clusters, since the shell effects diminish with increasing size. Indeed, several studies have been carried out with this method addressing the asymptotic behavior of ground-state properties towards the behavior of a jellium sphere of infinite size.[37–40]

It has been observed,[7,41–43] however, that the single-particle potentials resulting from the semiclassical method are very close, even for small cluster sizes, to those obtained via a self-consistent solution of the local-density-functional approximation (LDA) using the Kohn-Sham (KS) equations.[44] These semiclassical potentials were used extensively to describe the optical (linear) response of spherical metal clusters, for small,[7,41,42] as well as larger sizes[43] (for an experimental review on optical properties, cf. Refs. 45 and 46). The results of this approach are consistent with time-dependent local-density-functional approximation (TDLDA) calculations which use the KS solutions.[6,47]

It is natural to explore the use of these semiclassical potentials, in the spirit of Strutinsky's approach, for evaluation of shell corrections in metal clusters of arbitrary size. The present work shows that this program can be carried out successfully. Particularly interesting and promising is the manner by which the shell corrections are introduced by us through the kinetic-energy term, instead of the traditional Strutinsky averaging procedure of the single-particle spectrum.[27–29] This is especially desirable, since—unlike the case of atomic nuclei – shell corrections for metal clusters determined by the traditional Strutinsky procedure result in total energies exhibiting substantial systematic deviations from the corresponding KS-LDA energies.

Our shell-correction method (SCM) for calculating the ground-state properties of a system has certain similarities to the Harris-functional method,[48] proposed as an alternative to the self-consistent solution of KS-LDA equations, which was recently applied to electronic structure calculations of condensed-phase and molecular systems.[49–51] The present method circumvents as well the self-consistent solution of the KS equations and thus has the advantage of a significant reduction in computational effort, while preserving the numerical accuracy. In particular, our calculations show that our method yields results which agree typically within 1% to 3% with those obtained by self-consistent solutions of the KS equations.

In Sec. II we discuss first Strutinsky's method developed in the context of nuclear physics. Subsequently, we introduce and discuss the shell-correction method for investigations of metal clusters.

In Sec. III we present an application of the SCM approach to investigations of the properties of anionic metal clusters. Specifically we report on systematic theoretical studies of the energetics and stability of multiply charged anionic metal clusters and deduce relationships predicting borders of stability as a function of the size and number of excess electrons (the cluster size required to stably bind a given number of excess electrons). Beyond the border of stability, we estimate the lifetimes for spontaneous electron emission (autodetachment) which takes place via tunneling through a Coulombic barrier, in analogy with the nuclear processes of proton and alpha radioactivities. Additionally, we assess the importance of shell effects and self-interaction corrections for anionic metal clusters studied by the local-density-functional method. Fission channels, which may compete with electron autodetachment, are studied for the case of doubly charged anions. In all calculations reported here, we limit ourselves to a jellium background with spherical symmetry, except when specifically noted. Effects due to deformations will be treated comprehensively in a forthcoming publication.[52]

Finally, we summarize our results in Sec. IV.

II. SEPARATION OF THE BINDING ENERGY INTO A SMOOTH PART AND A SHELL CORRECTION

A. Shell-correction method in nuclear physics

1. Strutinsky's averaging of the single-particle spectra: Decomposition of the total energy into a smooth and a fluctuating (shell-correction) part

In their studies,[28,29] Strutinsky and collaborators worked with the Hartree-Fock (HF) theory, commonly used to represent the self-consistent field of atomic nuclei. While in reviewing Strutinsky's method we keep referring to the HF theory, the general form of the results is equally applicable, as we discuss below, to the density-functional theory commonly used in electronic structure calculations with a local approximation for the exchange-correlation functional.

Motivated by the behavior of the empirical nuclear binding energies, Strutinsky conjectured that the self-consistent Hartree-Fock density $\rho_{\rm HF}$ can be decomposed into a smooth density $\widetilde{\rho}$ and a fluctuating contribution $\delta\rho$, namely $\rho_{\rm HF} = \widetilde{\rho} + \delta\rho$. Then, he proceeded to show that, to second-order in $\delta\rho$, the Hartree-Fock energy is equal to the result that the same Hartree-Fock expression yields when $\rho_{\rm HF}$ is replaced by the smooth density $\widetilde{\rho}$ and the Hartree-Fock single-particle energies $\varepsilon_i^{\rm HF}$ are replaced by the single-particle energies corresponding to the smooth potential constructed with the smooth density $\widetilde{\rho}$. Namely, he showed that

$$E_{\rm HF} = E_{\rm Str} + O(\delta\rho^2) \ , \tag{1}$$

where the Hartree-Fock energy is given by the expression

$$E_{\rm HF} = \sum_i \varepsilon_i^{\rm HF} - \tfrac{1}{2}\int d\mathbf{r}\, d\mathbf{r}'\mathcal{V}(\mathbf{r}-\mathbf{r}')[\rho_{\rm HF}(\mathbf{r},\mathbf{r})\rho_{\rm HF}(\mathbf{r}',\mathbf{r}') - \rho_{\rm HF}(\mathbf{r},\mathbf{r}')^2] \ , \tag{2}$$

while the Strutinsky approximate energy is written as follows:

$$E_{\rm Str} = \sum_i \widetilde{\varepsilon}_i - \tfrac{1}{2}\int d\mathbf{r}\, d\mathbf{r}'\mathcal{V}(\mathbf{r}-\mathbf{r}')[\widetilde{\rho}(\mathbf{r},\mathbf{r})\widetilde{\rho}(\mathbf{r}',\mathbf{r}') - \widetilde{\rho}(\mathbf{r},\mathbf{r}')^2] \ . \tag{3}$$

The index i in Eq. (2) and Eq. (3) runs only over the occupied states (spin degeneracy is naturally implied). The single-particle energies $\widetilde{\varepsilon}_i$ correspond to a smooth potential $\widetilde{U}$. Namely, they are eigenvalues to a Schrödinger equation,

$$\left(-\frac{\hbar^2}{2m}\nabla^2 + \widetilde{U}\right)\varphi_i = \widetilde{\varepsilon}_i\varphi_i \ , \tag{4}$$

where the smooth potential $\widetilde{U}$ depends on the smooth density $\widetilde{\rho}$ as follows:

$$\widetilde{U}(\mathbf{r})\varphi_i(\mathbf{r}) = \int d\mathbf{r}'\mathcal{V}(\mathbf{r}-\mathbf{r}')[\widetilde{\rho}(\mathbf{r}',\mathbf{r}')\varphi_i(\mathbf{r}) - \widetilde{\rho}(\mathbf{r}',\mathbf{r})\varphi_i(\mathbf{r}')] \ , \tag{5}$$

and $\mathcal{V}$ is the nuclear two-body interaction potential.

Since the second term in Eq. (3) is a smooth quantity, Eq. (1) states that all shell corrections are, to first order in $\delta\rho$, contained in the sum of the single-particle energies $\sum_i \widetilde{\varepsilon}_i$. This is very useful, since it allows one to approximate the shell effects through the so-called Strutinsky averaging method. According to this method, a smooth part $\widetilde{E}_{\rm sp}$, is extracted out of the sum of the single-particle energies $\sum_i \widetilde{\varepsilon}_i$ by averaging them through an appropriate procedure. Usually, but not necessarily, one replaces the δ functions in the single-particle density of states by Gaussians or other appropriate weighting functions. As a result, each single-particle level is assigned an averaging occupation number $\widetilde{f}_i$, and the smooth part $\widetilde{E}_{\rm sp}$ is formally written as

$$\widetilde{E}_{\rm sp} = \sum_i \widetilde{\varepsilon}_i\widetilde{f}_i \ . \tag{6}$$

Consequently, the Strutinsky shell correction is given by

$$\Delta E_{\rm sh}^{\rm Str} = \sum_i \widetilde{\varepsilon}_i - \widetilde{E}_{\rm sp} \ . \tag{7}$$

The Strutinsky prescription (7) has the practical advantage of using only the single-particle energies $\widetilde{\varepsilon}_i$ and not the smooth density $\widetilde{\rho}$. Taking advantage of this, the single-particle energies can be taken as those of any external potential that empirically approximates the self-consistent potential of a small system. In the nuclear case, an anisotropic three-dimensional harmonic oscillator has been used successfully to describe the shell corrections in deformed nuclei.

The single-particle smooth part $\widetilde{E}_{\rm sp}$, however, is only one component of the total smooth contribution, $\widetilde{E}_{\rm HF}$, in the Hartree-Fock energy. Indeed as can be seen from Eq. (3),

$$E_{\rm HF} \approx \Delta E_{\rm sh}^{\rm Str} + \widetilde{E}_{\rm HF} \ , \tag{8}$$

where

$$\widetilde{E}_{\rm HF} = \widetilde{E}_{\rm sp} - \tfrac{1}{2}\int d\mathbf{r}\, d\mathbf{r}'\mathcal{V}(\mathbf{r}-\mathbf{r}')[\widetilde{\rho}(\mathbf{r},\mathbf{r})\widetilde{\rho}(\mathbf{r}',\mathbf{r}') - \widetilde{\rho}(\mathbf{r},\mathbf{r}')^2] \ . \tag{9}$$

Strutinsky did not address the question of how to calculate microscopically the smooth part $\widetilde{E}_{\rm HF}$ (which necessarily entails specifying the smooth density $\widetilde{\rho}$). Instead he circumvented this question by substituting for $\widetilde{E}_{\rm HF}$ the empirical energies $E_{\rm LD}$ of the nuclear liquid-drop model; namely, he suggested that

$$E_{\rm HF} \approx \Delta E_{\rm sh}^{\rm Str} + E_{\rm LD} \ . \tag{10}$$

This last approximation has been very successful in describing fission barriers and properties of strongly deformed nuclei.

2. *Extended Thomas-Fermi method for the smooth contribution*

The success of Strutinsky's approximation (10) in nuclear physics has been impressive. It was, however, natural to inquire about the smooth density $\widetilde{\rho}$ and about ways of specifying it while circumventing the HF solution. Before proceeding further in this direction, we note that in most nuclear physics studies the HF theory is used in conjunction with effective forces of the Skyrme type.[53] The introduction of these forces builds correlation effects into the HF approach. Consequently, the resulting HF equations, with the effective fields expressed as functional derivatives of a parametrized energy density functional, are equivalent to the KS equations of DFT, generalized to include nonlocal parts of the potential.[54]

It was observed that not only $\sum_i \widetilde{\varepsilon}_i$ but also most HF quantities can be averaged in the Strutinsky sense. In particular, using the Strutinsky averaging occupation numbers [$\widetilde{f}_i$, see Eq. (6)], one can extract averages for the HF density and the Hartree-Fock kinetic energy, namely

$$\widetilde{\rho} = \sum_i |\phi_i^{\mathrm{HF}}|^2 \widetilde{f}_i \tag{11}$$

and

$$\widetilde{T} = -\frac{\hbar^2}{2m} \sum_i \langle \phi_i^{\mathrm{HF}} | \nabla^2 | \phi_i^{\mathrm{HF}} \rangle \widetilde{f}_i \ . \tag{12}$$

A different approach than Eq. (11) for specifying the single-particle density of a quantal system in an average sense has been initiated by Thomas and Fermi.[55] In its modern version, it is known as the extended Thomas Fermi (ETF) method. In this approach,[56] the full quantum-mechanical single-particle density is written as an inverse Laplace transform ($\mathcal{L}_\lambda^{-1}$, where λ is the Fermi energy) of the Bloch density matrix

$$C(\mathbf{r}, \mathbf{r}'; \beta) = \sum_i \varphi_i^*(\mathbf{r}') \varphi_i(\mathbf{r}) \exp(-\beta \varepsilon_i) \ . \tag{13}$$

Namely,

$$\rho(\mathbf{r}, \mathbf{r}') = \mathcal{L}_\lambda^{-1} \left[\frac{1}{\beta} C(\mathbf{r}, \mathbf{r}'; \beta) \right] \ . \tag{14}$$

Expanding[57] $C(\mathbf{r}, \mathbf{r}'; \beta)$ in powers of $\hbar$, one obtains a semiclassical density ρ_{ETF} in powers of $\hbar$. More importantly for our purposes, the corresponding approximation of the kinetic energy T_{ETF} is given as a density functional of ρ_{ETF}, and thus ρ_{ETF} can be determined as the solution of a variational Euler-Lagrange equation.

It was natural to inquire whether the Strutinsky smooth density $\widetilde{\rho}$ and ρ_{ETF} (both obtained for the same density-dependent potential-energy terms) are connected in any way. In fact, through direct numerical comparison, it was found[31,32] that practically $\widetilde{\rho} = \rho_{\mathrm{ETF}}$ (as well as $\widetilde{T} = T_{\mathrm{ETF}}$), provided that the ETF kinetic-energy functional was specified up to the fourth order in the gradient expansion.

Due to the availability of reliable empirical liquid-drop energies, the Strutinsky ansatz (10) has been used in most nuclear studies, with the ETF approach finding only limited application. However, in the case of metal clusters, the ETF approach for specifying the smooth part appears to be a natural starting point in adapting Strutinsky' s method to these systems.

B. Adaptation of the shell-correction method to metal clusters

1. *Extended Thomas-Fermi method for the smooth contribution in metal clusters*

As mentioned above, self-consistent solutions of the Kohn-Sham equations are commonly used to calculate properties of metal clusters. Alternatively, an ETF method in conjuction with the local-density approximation for exchange and correlation, based on a variational procedure using a parametrized density profile, has also been used.[34–36,7,41,42] In our calculations, we use

$$\rho(r) = \frac{\rho_0}{\left[1 + \exp\left(\frac{r - r_0}{\alpha}\right)\right]^\gamma} \ , \tag{15}$$

with r_0, α, and γ as variational parameters (for other closely related parametrizations cf. Refs. 34 and 36). The energy density functional, namely

$$E[\rho] = \int \left(t[\rho(\mathbf{r})] + \{ \tfrac{1}{2} V_H[\rho(\mathbf{r})] + V_I(\mathbf{r}) \} \rho(\mathbf{r}) \right) d\mathbf{r} + \int \mathcal{E}_{\mathrm{xc}}[\rho(\mathbf{r})] d\mathbf{r} + E_I \ , \tag{16}$$

that is variationally minimized consists of a kinetic-energy functional $t[\rho]$, specified according to the ETF theory (comprising terms up to fourth order in the density gradients[56]), and of Hartree (H) and exchange-correlation functionals [(xc), for the latter we use the Gunnarsson-Lundqvist functional.[58]] V_H is the Hartree repulsive potential induced by the electrons. V_I and E_I are the attractive potential and the repulsive total electrostatic energy of the positive jellium background. The *smooth* optimal electronic density $\widetilde{\rho}$, obtained through a variational minimization of this ETF functional [Eqs. (15) and (16)] is input into Eq. (16) to yield the smooth part $\widetilde{E}[\widetilde{\rho}]$ of the total energy of the cluster.

With this density, the LDA average potential, $\widetilde{U}(\mathbf{r}; \widetilde{\rho}(\mathbf{r}))$, binding the delocalized electrons, consists of a sum of three terms; a repulsive Hatree term and an attractive exchange-correlation term from the electronic contribution, as well as an electrostatic term originating from the attraction between the electrons and the positively charged jellium background, namely

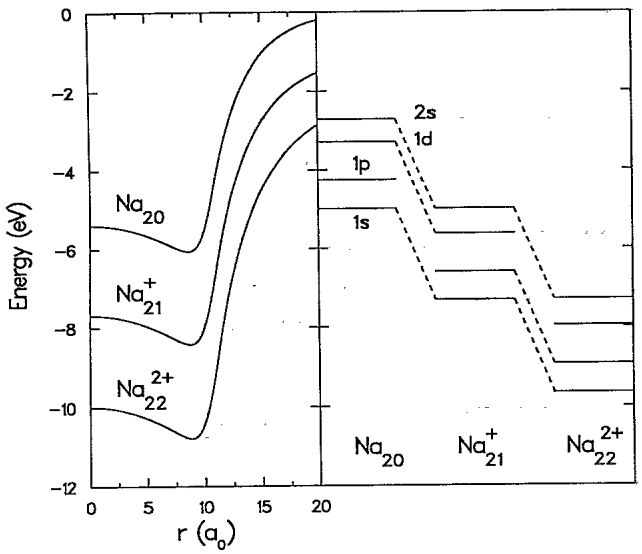

FIG. 1. ETF effective potentials for Na_{20}, Na_{21}^{+}, and Na_{22}^{2+} in the spherical jellium background approximation. The associated single-particle occupied levels are also shown. Observe the increasing depth of the potentials with increasing total cationic charge. Distances are in units of the Bohr radius a_0.

$$\widetilde{U}(\mathbf{r};\widetilde{\rho}(\mathbf{r})) = 2\int \frac{\widetilde{\rho}(\mathbf{r}')}{|\mathbf{r}-\mathbf{r}'|}d\mathbf{r}' + \widetilde{V}_{\rm xc}(\mathbf{r};\widetilde{\rho}(\mathbf{r})) + V_I(\mathbf{r}) \ , \quad (17)$$

where atomic units (energy in Ry) are implied. In our calculations, the exchange-correlation potential $V_{\rm xc}(\mathbf{r}) \equiv \delta\mathcal{E}_{\rm xc}\rho(\mathbf{r})/\delta\rho(\mathbf{r})$ is given by the expression

$$V_{\rm xc}(\mathbf{r}) = -1.222/r_s(\mathbf{r}) - 0.0666\ln\left(1+\frac{11.4}{r_s(\mathbf{r})}\right) \ , \quad (18)$$

where $r_s(\mathbf{r}) = [3/4\pi\widetilde{\rho}(\mathbf{r})]^{1/3}$ is the local value of the Wigner-Seitz radius.

Having obtained the effective potential $\widetilde{U}(\mathbf{r};\widetilde{\rho}(\mathbf{r}))$, one proceeds to calculate the electronic single-particle spectrum by solving Schrödinger's equation using the one-particle Hamiltonian,

$$H_0 = \widehat{T} + \widetilde{U}(\mathbf{r};\widetilde{\rho}(\mathbf{r})) \ , \quad (19)$$

where $\widehat{T}$ is the quantum-mechanical operator for the kinetic energy.

An example of these effective potentials and of the associated occupied single-particle spectra is given in Fig. 1. We have chosen to exhibit the case of Na_{20}, Na_{21}^{+}, and Na_{22}^{2+}. In all three cases, 20 delocalized electrons are involved, but the corresponding potentials become successively deeper as one passes from the neutral to the doubly cationic case.

2. *Shell correction through the kinetic-energy term*

Motivated by the analogies between certain properties of nuclei and metal clusters, in particular the oscillatory behavior of ground-state properties as a function of size, we conjecture that the main conclusion of Strutinsky's theorem (derived originally in the context of HF calculations) can be applied as well to metal clusters, in the context of local-density-functional theory. Namely, we assert (for a justification, see Sec. II B 3) that the shell effects in the total energy of a metal cluster are, to the first order in $\delta\rho_{\rm KS}$ (where $\delta\rho_{\rm KS} = \rho_{\rm KS} - \widetilde{\rho}$, and $\rho_{\rm KS}$ is the self-consistent KS density), contained in the sum $\sum_i \widetilde{\varepsilon}_i$, where $\widetilde{\varepsilon}_i$ are the single-particle energies of the effective potential $\widetilde{U}(\mathbf{r};\widetilde{\rho}(\mathbf{r}))$ constructed according to Eq. (17). In the expression for the smooth total energy $\widetilde{E}$ [the energy density functional (16) evaluated for $\rho = \widetilde{\rho}$], the term that can be related to this sum is the kinetic-energy contribution. Indeed, the quantal kinetic energy of particles moving independently in an effective potential can be expressed as the sum over single-particle energies minus a potential-energy term. Since $\sum_i \widetilde{\varepsilon}_i$ is already first order in $\delta\rho_{\rm KS}$, the potential-energy term must be approximated by its smooth part for our purposes here. Thus we are led to replace $\widetilde{T} = \int \widetilde{t}[\widetilde{\rho}(\mathbf{r})]d\mathbf{r}$ in the ETF functional (16) by the expression

$$T_{\rm sh} = \sum_i \widetilde{\varepsilon}_i - \int \widetilde{\rho}(\mathbf{r})\widetilde{U}(\mathbf{r};\widetilde{\rho}(\mathbf{r}))d\mathbf{r} \ . \quad (20)$$

As a result, the total energy $E_{\rm sh}$, including the shell correction,

$$\Delta E_{\rm sh} = T_{\rm sh} - \widetilde{T} \ , \quad (21)$$

is given by

$$E_{\rm sh}[\widetilde{\rho}] = T_{\rm sh} - \widetilde{T} + \widetilde{E}[\widetilde{\rho}] \ . \quad (22)$$

After some rearrangenments, the shell-corrected total energy $E_{\rm sh}[\widetilde{\rho}]$ in Eq. (22) can be written in functional form as follows:

$$E_{\rm sh}[\widetilde{\rho}] = \sum_i \widetilde{\varepsilon}_i - \int [\tfrac{1}{2}\widetilde{V}_H(\mathbf{r}) + \widetilde{V}_{\rm xc}(\mathbf{r})]\widetilde{\rho}(\mathbf{r})d\mathbf{r} + \int \widetilde{\mathcal{E}}_{\rm xc}[\widetilde{\rho}(\mathbf{r})]d\mathbf{r} + E_I \ . \quad (23)$$

As with the Strutinsky method in nuclear physics, the total energy $E_{\rm sh}$, as well as the shell correction $\Delta E_{\rm sh}$, is expressed *solely* through the *smooth* density $\widetilde{\rho}$, without the need to evaluate the self-consistent Kohn-Sham density $\rho_{\rm KS}$. This method thus circumvents the solution of the KS eigenvalue problem at each step of the iteration procedure performed to achieve self-consistency in the single-particle wave functions. In our method, a matrix eigenvalue equation is solved only once following the ETF variation which determines the smooth density $\widetilde{\rho}$. We further note that the calculation of the total energy $E_{\rm sh}$ (or the shell correction $\Delta E_{\rm sh}$) requires only the eigenvalues $\widetilde{\varepsilon}_i$, and not the corresponding eigenvectors $\widetilde{\psi}_i(\mathbf{r})$.

To check the accuracy of this procedure, we have compared results of calculations using the functional $E_{\rm sh}$ [Eq. (22)] with available Kohn-Sham calculations. In particular, Fig. 2 displays results of the present shell-correction

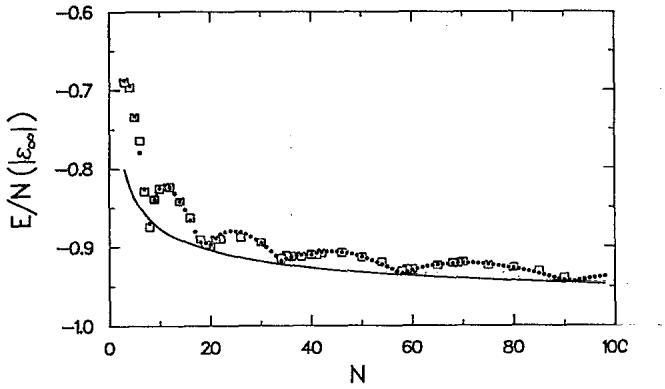

FIG. 2. Total energy per atom of neutral sodium clusters (in units of the absolute value of the energy per atom in the bulk, $|\varepsilon_\infty| = 2.252$ eV). Solid circles: SCM results (see the text for details). The solid line is the ETF result (smooth contribution). In both cases, a spherical jellium background was used. Open squares: LDA Kohn-Sham results from Ref. 19. The excellent agreement (a discrepancy of only 1–3 %) between the SCM and the LDA Kohn-Sham approach is to be stressed.

approach for the total energies of neutral sodium clusters. The results of the shell-correction method for ionization potentials of sodium clusters are displayed in Fig. 3. The excellent agreement between the oscillating results obtained via our theory and the Kohn-Sham results (cf., e.g., Ref. 19) is evident. To further illustrate the two components (smooth contribution and shell correction) entering into our approach, we also display the smooth parts resulting from the ETF method.

3. Connection to the Harris functional

The excellent numerical agreement illustrated above suggests that the Strutinsky theorem (1) can be *proven*, not only for the Hartree-Fock, but also for the case of the density-functional theory, namely

$$E_{\rm KS}[\rho_{\rm KS}] = E_{\rm sh}[\tilde{\rho}] + O(\delta\rho_{\rm KS}^2) \ . \tag{24}$$

Indeed, several recent publications have proven[51,49,59] the validity of Eq. (24) in connection with the Harris[48] functional, used in electronic structure calculations of molecules, surfaces, and other condensed-matter systems. In fact, the specific way of writing the functional (23) was chosen so that its similarity in form to the Harris functional is evident. Formally, the Harris functional $E_{\rm Harris}[\rho_{\rm in}]$ results from expression (23) by replacing the smooth density $\tilde{\rho}$ by an *input* density $\rho_{\rm in}$, taken as a superposition of site densities. Initially[48] the site components of the input density were not optimized. Later,[49,59] it was realized that the results could be improved by variationally adjusting the site components through a *maximization* of the Harris functional itself. However, doing so adds the burden of a matrix diagonalization for obtaining the eigenvalues ε_j at each step of the variation. We note that our method differs from the Harris approach in that the optimization of the input density is achieved by us through a variational ETF method,[60] which does not require such a step-by-step matrix diagonalization. While our focus in this paper is on jellium models for metal clusters, the very good agreement between our results and those obtained via KS self-consistent jellium calculations suggests that it would be worthwhile to explore the application of our method to more general electronic structure calculations extending beyond the jellium model, where the trial density used for minimization of the ETF functional could be taken as a superposition of site densities, as in the Harris method. Additionally, application of our method to nuclear HF-Skyrme calculations is suggested.

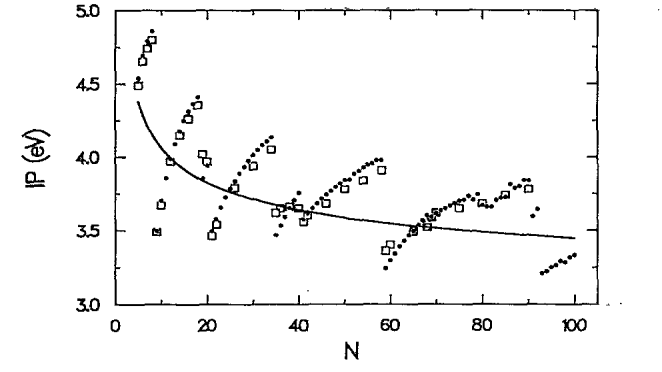

FIG. 3. Ionization potentials (IP's) for sodium clusters. Solid circles: IP's calculated with the SCM (see the text for details). The solid line corresponds to the ETF results (smooth contribution). In both cases, a spherical jellium background was used. Open squares: LDA Kohn-Sham results from Ref. 19. The excellent agreement (a discrepancy of only 1–3 %) between the shell-correction method and the full Kohn-Sham approach should be noted.

III. MULTIPLY CHARGED METAL-CLUSTER ANIONS

Charging of large metal spheres is an old subject with scientific accounts dating back to Coulomb, Faraday, and others.[61] While size-evolutionary patterns of physical and chemical properties of finite clusters, neutral as well as cationic, have been the subject of intensive research,[2,3,62] negatively charged metal clusters have not been as much investigated, with the exception of several experimental and theoretical studies concerning singly charged anions.[63–67,42,68]

As mentioned above, investigations of metal clusters based on LDA methods and self-consistent solutions of the Kohn-Sham equations (employing either a positive jellium background or maintaining the discrete ionic cores) have contributed significantly to our understanding of these systems.[2,8,19,22] However, even for singly negatively charged metal clusters (M_N^-), difficulties may arise due to the failure of the solutions of the KS equations to converge, since the eigenvalue of the excess electron may iterate to a positive energy.[69] While such difficulties are alleviated for M_N^- clusters via self-interaction

corrections (SIC),[70,18] the treatment of multiply charged clusters (M_N^{Z-}, $Z > 1$) would face similar difficulties in the metastability region against electronic autodetachment through a Coulombic barrier. In the following we are applying our SCM approach, described in Sec. II B, to these systems (for the jellium background, we assume spherical symmetry, unless otherwise stated).

A. Electron affinities and borders of stability

The smooth multiple electron affinities $\widetilde{A}_Z$ prior to shell corrections are defined as the difference in the total energies of the clusters

$$\widetilde{A}_Z = \widetilde{E}(vN, vN+Z-1) - \widetilde{E}(vN, vN+Z)\,, \qquad (25)$$

where N is the number of atoms, v is the valency, and Z is the number of excess electrons in the cluster (e.g., first and second affinities correspond to $Z=1$ and $Z=2$, respectively). vN is the total charge of the positive background. Applying the shell correction (21), we calculate the full electron affinity as

$$A_Z^{\rm sh} - \widetilde{A}_Z = \Delta E_{\rm sh}(vN, vN+Z-1) - \Delta E_{\rm sh}(vN, vN+Z)\,. \qquad (26)$$

A positive value of the electron affinity indicates stability upon attachment of an extra electron. Figure 4 displays the smooth, as well as the shell-corrected, first and second electron affinities for sodium clusters with $N < 100$. Note that $\widetilde{A}_2$ becomes positive above a certain critical size, implying that the second electron in doubly negatively charged sodium clusters with $N < N_{\rm cr}^{(2)} = 43$ might not be stably attached. The shell effects, however, create two islands of stability about the magic clusters Na_{32}^{2-} and Na_{38}^{2-} (see $A_2^{\rm sh}$ in Fig. 4). To predict the critical cluster size $N_{\rm cr}^{(Z)}$, which allows the stable attachment of Z excess electrons, we calculated the smooth electron affinities of sodium clusters up to $N = 255$ for $1 \le Z \le 4$, and display the results in Fig. 5. We observe that $N_{\rm cr}^{(3)} = 205$, while $N_{\rm cr}^{(4)} > 255$.

The similarity of the shapes of the curves in Fig. 5, and the regularity of distances between them, suggest that the smooth electron affinities can be fitted by a general expression of the form

$$\widetilde{A}_Z = \widetilde{A}_1 - \frac{(Z-1)e^2}{R+\delta} = W - \beta\frac{e^2}{R+\delta} - \frac{(Z-1)e^2}{R+\delta}, \qquad (27)$$

where the radius of the positive background is $R = r_s N^{1/3}$. From our fit, we find that the constant W corresponds to the bulk work function. In all cases, we find $\beta = 5/8$, which suggests a close analogy with the classical model of the image charge.[71,72] For the spill-out parameter, we find a weak size dependence as $\delta = \delta_0 + \delta_2/R^2$. The contribution of δ_2/R^2, which depends on Z, is of importance only for smaller sizes and does not affect substantially the critical sizes (where the curve crosses the zero line), and consequently δ_2 can be neglected in such estimations. Using the values obtained by us for $\widetilde{A}_1$ of

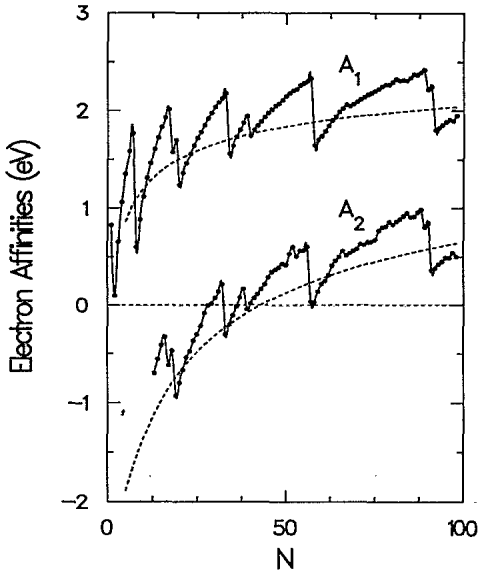

FIG. 4. Calculated first (A_1) and second (A_2) electron affinities of sodium clusters as a function of the number of atoms N. Both their smooth part (dashed lines) and the shell-corrected affinities (solid circles) are shown. A spherical jellium background was used.

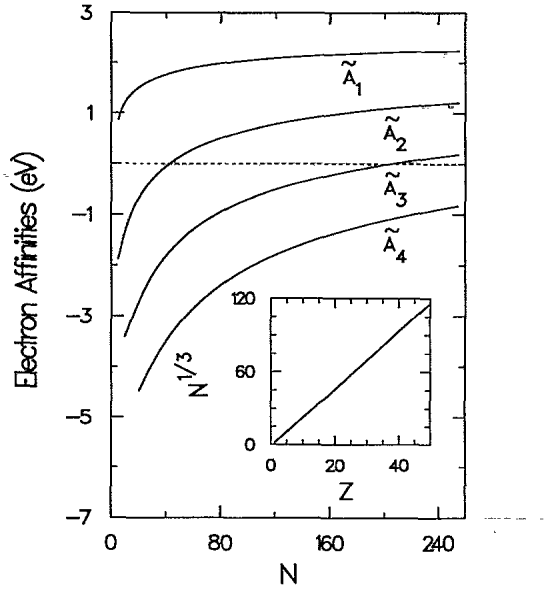

FIG. 5. Calculated smooth electron affinities $\widetilde{A}_Z$, $Z = 1$–4, for sodium clusters as a function of the number of atoms N (Z is the number of excess electrons). A spherical jellium background was used. Inset: The electron *drip* line for sodium clusters. Clusters stable against spontaneous electron emission are located above this line. While, as seen from Fig. 4 for spherical geometry, shell effects influence the border of stability, shell-corrected calculations including deformations (Ref. 52) yield values close to the drip line (shown in the inset) which was obtained from the smooth contributions.

sodium clusters (namely, $W = 2.9$ eV, which is also the value obtained by KS-LDA calculations for an infinite planar surface,[73] $\delta_0 = 1.16$ a.u., with $R = r_s N^{1/3}$ and $r_s = 4.00$ a.u.), we find for the critical sizes when the left-hand side of Eq. (27) is set equal to zero, $N_{\rm cr}^{(2)} = 44$, $N_{\rm cr}^{(3)} = 202$, $N_{\rm cr}^{(4)} = 554$, and $N_{\rm cr}^{(5)} = 1177$, in very good agreement with the values obtained directly from Fig. 5.

The curve that specifies $N_{\rm cr}^{(Z)}$ in the (Z, N) plane defines the border of stability for spontaneous electron decay. In nuclei, such borders of stability against spontaneous proton or neutron emission are known as nucleon drip lines.[74] For the case of sodium clusters, the electron drip line is displayed in the inset of Fig. 5.

B. Metastability against electron autodetachment

The multiply charged anions with negative affinities do not necessarily exhibit a positive total energy. To illustrate this point, we display in Fig. 6 the calculated total energies per atom $[\widetilde{E}(N,Z)/N]$ as a function of excess charge (Z) for clusters containing 30, 80, and 240 sodium atoms. These sizes allow for exothermic attachment of maximum one, two, or three excess electrons, respectively.

As was the case with the electron affinities, the total-energy curves in Fig. 6 show a remarkable regularity, suggesting a parabolic dependence on the excess charge. To test this conjecture, we have extracted from the calculated total energies the quantity $g(N,Z) = G(N,Z)/N$, where $G(N,Z) = [\widetilde{E}(N,Z) - \widetilde{E}(N,0)]/Z + \widetilde{A}_1(N)$, and have plotted it in the inset of Fig. 6 as a function of the excess negative charge Z. The dependence is linear to a remarkable extent; for $Z = 1$ all three lines cross the energy axis at zero. Combined with the results on the electron affinities, this indicates that the total energies have the following dependence on the excess number of electrons (Z):

$$\widetilde{E}(Z) = \widetilde{E}(0) - \widetilde{A}_1 Z + \frac{Z(Z-1)e^2}{2(R+\delta)}, \tag{28}$$

where the dependence on the number of atoms in the cluster is not explicitly indicated.

This result is remarkable in its analogy with the classical image-charge result of van Staveren *et al.*[72] Indeed, the only difference amounts to the spill-out parameter δ_0 and to the weak dependence on Z through δ_2. This additional Z dependence becomes negligible already for the case of 30 sodium atoms.

For metastable multiply charged cluster anions, electron emission (autodetachment) will occur via tunneling through a barrier (shown in Fig. 7). However, to reliably estimate the electron emission, it is necessary to correct the LDA effective potential for self-interaction effects. We performed a self-interaction correction of the Amaldi type[69] for the Hartree term and extended it to

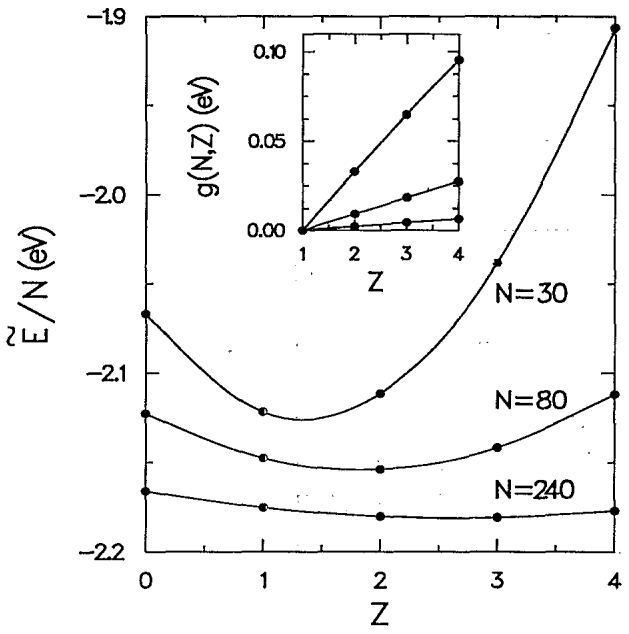

FIG. 6. Calculated smooth total energy per atom as a function of the excess negative charge Z for the three families of sodium clusters with $N = 30$, $N = 80$, and $N = 240$ atoms. A spherical jellium background was used. As the straight lines in the inset demonstrate, the curves are parabolic. We find that they can be fitted by Eq. (28). See text for an explanation of how the function $g(N,Z)$ was extracted from the calculations.

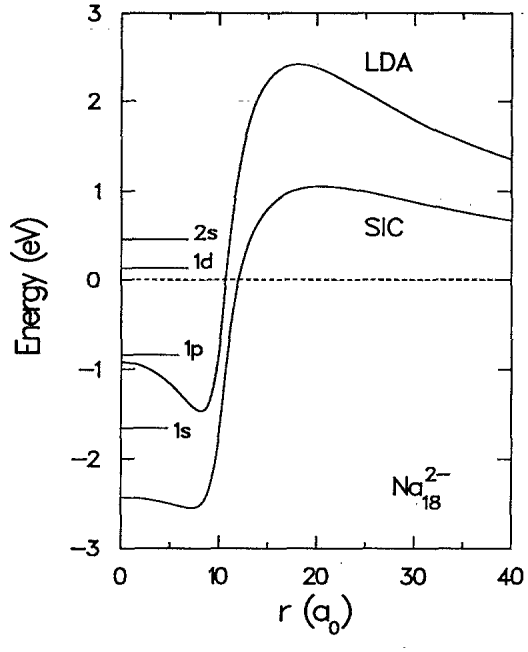

FIG. 7. The LDA and the corresponding self-interaction corrected (SIC) potential for the metastable Na_{18}^{2-} cluster. A spherical jellium background was used. The single-particle levels of the SIC potential are also shown. Unlike the LDA, this latter potential exhibits the correct asymptotic behavior. The $2s$ and $1d$ electrons can be emitted spontaneously by tunneling through the Coulombic barrier of the SIC potential. Distances are in units of the Bohr radius a_0.

the exchange-correlation contribution to the total energy as follows: $E_{\rm xc}^{\rm SIC}[\rho] = E_{\rm xc}^{\rm LDA}[\rho] - N_e E_{\rm xc}^{\rm LDA}[\rho/N_e]$, where $N_e = vN + Z$ is the total number of electrons. This self-interaction correction is akin to the orbitally-averaged potential method.[69] Minimizing the SIC energy functional for the parameters r_0, α, and γ, we obtained the effective SIC potential for Na_{18}^{2-} shown in Fig. 7, which exhibits the physically correct asymptotic behavior.[75]

The spontaneous electron emission through the Coulombic barrier is analogous to that occurring in proton radioactivity from neutron-deficient nuclei,[76] as well as in alpha-particle decay. The transition rate is $\lambda = \ln 2/T_{1/2} = \nu P$, where ν is the attempt frequency and P is the transmission coefficient calculated in the WKB method (for details, cf. Ref. 76). For the $2s$ electron in Na_{18}^{2-} (cf. Fig. 7), we find $\nu = 0.73 \times 10^{15}$ Hz and $P = 4.36 \times 10^{-6}$, yielding $T_{1/2} = 2.18 \times 10^{-10}$ s. For a cluster size closer to the drip line (see Fig. 5), e.g., Na_{35}^{2-}, we find $T_{1/2} = 1.13$ s.

C. Fission of doubly charged anions

As is the case of doubly charged cations, doubly charged anions may fission. Thus the fission channel may compete with the spontaneous electron emission one. Using the shell-correction method, we calculated the dissociation energies $\Delta_P^{\rm neg} = E_{\rm sh}(Na_P^-) + E_{\rm sh}(Na_{N-P}^-) - E_{\rm sh}(Na_N^{2-})$ as a function of parent size N and daughter products P and $N - P$. Spherical symmetry was assumed for both parents and daughters. The dissociation energies $\Delta_f^{\rm neg}$ for the most favorable channels, i.e., for the smallest $\Delta_P^{\rm neg}$ for a given N, are displayed in Fig. 8. For comparison with the case of doubly positive cationic parents, we have calculated as well the dissociation energies $\Delta_P^{\rm pos} = E_{\rm sh}(Na_P^+) + E_{\rm sh}(Na_{N-P}^+) - E_{\rm sh}(Na_N^{2+})$ and have plotted the corresponding energies for the most favorable channels, $\Delta_f^{\rm pos}$, in Fig. 9. Again, comparison of the results in Fig. 9 with the results of Ref. 11 (calculated using the KS equations) illustrates the high degree of accuracy of the SCM approach introduced in this work.

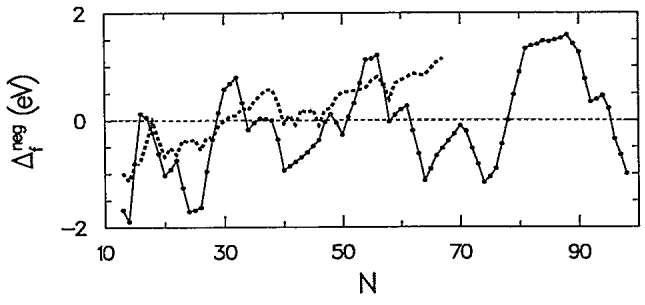

FIG. 8. Solid circles: SCM results for the dissociation energies $\Delta_f^{\rm neg}$ for the most favorable fission channel for doubly charged anionic parents Na_N^{2-} when the spherical jellium is used. The influence of deformation effects is shown by the thick dashed line. Table I lists the composition of the most favorable channels.

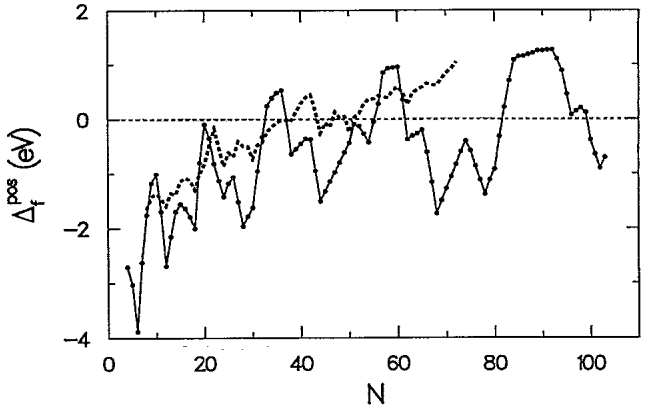

FIG. 9. Solid circles: SCM results for the dissociation energies $\Delta_f^{\rm pos}$ for the most favorable fission channel for doubly charged cationic parents Na_N^{2+} when the spherical jellium is used. The excellent agreement between the shell-correction method and the LDA Kohn-Sham approach (cf., e.g., Ref. 11) is evident. The influence of deformation effects is shown by the thick dashed line. Table I lists the composition of the most favorable channels.

The patterns exhibited by the favorable channels in the case of doubly negative parents (plotted as energy versus the number of atoms in the parent cluster) are similar to those exhibited by the doubly positive parents,[11] apart from a natural shift of four mass units. In particular, magic parents are the least favored to fission, exhibiting typically endothermic behavior. All favorable channels contain at least one magic fragment, with the local minima corresponding to two magic daughters. Table I summarizes the composition of favorable channels up to $N = 20$.

As was the case with the doubly cationic parents, the local minima of $\Delta_f^{\rm neg}$ for the doubly anionic parents remain strongly exothermic even for sizes up to $N = 100$ atoms, suggesting that the critical number N_c^F for fission above which Coulomb explosion, that is spontaneous fission, will not occur (namely $\Delta_f > 0$ for all N such that $N > N_c^F$) may be larger than 100. However, deformation effects can alter some conclusions drawn from shell effects derived from the spherical jellium. To check this possibility, we have applied the shell-correction method to fully triaxial deformed shapes. Some first results for both the doubly negative and doubly positive parents are displayed in Fig. 8 and Fig. 9 by a thick dashed line.[77] The main difference from the spherical jellium is a strong suppression of the local minima, indicating that N_c^F may be significantly smaller than 100, as indeed has been observed experimentally for hot cationic alkali-metal clusters.[9] From Fig. 8 we observe that for doubly charged anionic clusters, Na_N^{2-} (for which $N_{\rm cr}^{(2)} \approx 43$), fission may compete with the electron decay channel for $N \leq 30$, while for $30 < N < 43$ the latter one dominates.

Additionally, compared to the spherical jellium, in several cases the deformation effects result in a different composition of the most favorable channel. Examples of such cases are given in Table I. It should be noticed that, unlike the case of the spherical jellium, the shell-

TABLE I. Energetically favorable channels for the fissioning processes $Na_N^{2+} \rightarrow Na_P^{+}+Na_{N-P}^{+}$ and $Na_N^{2-} \rightarrow Na_P^{-}+Na_{N-P}^{-}$. S denotes the case in which both parents and daughters are assumed spherical. D denotes the case in which triaxial deformations are allowed for open-shell clusters (either parents and/or daughters). A dash denotes no change in the favorable channel.

Cations			Anions		
Parent (N)	Daughters (P, $N-P$)		Parent (N)	Daughters (P, $N-P$)	
	S	D		S	D
4	(1,3)	—			
5	(2,3)	—			
6	(3,3)	—			
7	(3,4)	—			
8	(3,5)	—			
9	(1,8)	(3,6)			
10	(1,9)	(3,7)			
11	(3,8)	—			
12	(3,9)	—			
13	(3,10)	(4,9)	13	(6,7)	—
14	(3,11)	(5,9)	14	(7,7)	—
15	(6,9)	—	15	(7,8)	—
16	(7,9)	—	16	(7,9)	—
17	(8,9)	—	17	(1,16)	(7,10)
18	(9,9)	—	18	(1,17)	(7,11)
19	(9,10)	—	19	(1,18)	—
20	(1,19)	(9,11)	20	(1,19)	—

correction method for deformed droplets predicts ($P = 3$, $N - P = 6$) and ($P = 3$, $N - P = 7$) to be the preferred channels for Na_9^{2+} and Na_{10}^{2+}, respectively, in agreement with the local-spin-density (LSD) functional molecular-dynamics calculation of fission patterns.[8]

D. Critical sizes for potassium and aluminum

While in this investigation we have used sodium clusters as a test system, the methodology and conclusions extend to other materials as well. Thus given a calculated or measured bulk work function W, and a spill-out parameter (δ_0 typically of the order of 1–2 a.u., and neglecting δ_2), one can use Eq. (27), with $\tilde{A}_Z = 0$, to predict critical sizes for other materials. For example, our calculations for potassium ($r_s = 4.86$ a.u.) give fitted values $W = 2.6$ eV [compared to a KS-LDA value of 2.54 eV for a semi-infinite planar surface with $r_s = 5.0$ a.u. (Ref. 73)] and $\delta_0 = 1.51$ a.u. for $\delta_2 = 0$, yielding $N_{\rm cr}^{(2)} = 33$, $N_{\rm cr}^{(3)} = 152$, and $N_{\rm cr}^{(4)} = 421$.

As a further example, we give our results for a trivalent metal, i.e., aluminum ($r_s = 2.07$ a.u.), for which our fitted values are $W = 3.65$ eV [compared to a KS-LDA value of 3.78 eV for a semi-infinite plane surface, with $r_s = 2.0$ a.u. (Ref. 73)] and $\delta_0 = 1.86$ a.u. for $\delta_2 = 0$, yielding $N_{\rm cr}^{(2)} = 40$ (121 electrons), $N_{\rm cr}^{(3)} = 208$ (626 electrons), and $N_{\rm cr}^{(4)} = 599$ (1796 electrons).

Finally, expression (28) for the total energy can be naturally extended to the case of multiply *positively* charged metal clusters by setting $Z = -z$, with $z > 0$. The ensuing equation retains the same dependence on the excess positive charge z, but with the negative value of the first affinity, $-\tilde{A}_1$, replaced by the positive value of the first ionization potential, $\tilde{I}_1 = W + (3/8)e^2/(R + \delta)$, a result that has been suggested from earlier measurements on multiply charged potassium cations.[78] Naturally, the spill-out parameter δ assumes different values than in the case of the anionic clusters.

IV. SUMMARY

Observations of size-evolutionary patterns of physical and chemical properties of clusters (that is, systematics of the variation of the properties of finite aggregates when recorded versus system size, e.g., the number of atoms) and analogies between such patterns and well-known SEP's of nuclear properties (e.g., binding energies or nuclear masses, recorded versus the number of nucleons), served as a principal motivation for the work reported in this paper. Based on the concept of decomposition of the size-dependent variation of the total energy of a finite system into a *smooth* part and a companion component, which adds a superimposed structure (shell correction) on the smooth curve, we were led to develop a method that allows time-efficient and accurate calculations of energetics and SEP's of the properties of metal clusters.

In our shell-correction method, the smooth component of the energy is determined via an optimization of an input density via variational treatment of the extended Thomas-Fermi (ETF) density functional (with the kinetic energy expanded to fourth order in the density gradients), and subsequent evaluation of the total energy with shell corrections introduced through the kinetic-energy term [see Sec. II B 2, Eqs. (20)–(23)], using the single-particle eigenvalues obtained via the solution of the Schrödinger equation within the LDA approximation

and using the ETF-optimized density.

While our original derivation of the method was partly motivated by studies of Strutinsky and collaborators in the context of nuclear physics, we discussed the similarity between our procedure and the Harris-functional method developed in the context of electronic structure calculations (see Sec. II B 3), which also attempts to circumvent self-consistent solutions to the Kohn-Sham LDA equations. We note, however, that our method utilizes a different optimization procedure of the input density, which allows for the matrix-diagonalization step to be performed once (after the optimization of the density is achieved via the ETF variational treatment), while in the Harris-functional approach maximization of the Harris functional requires diagonalization at each step of the variation.

To demonstrate the method, we calculated binding energies and ionization potentials of Na_N ($N \leq 100$) clusters, modeled as jellium droplets, exhibiting shell-structure effects, and obtaining excellent agreement with available self-consistent LDA results and experimental data.

Our main focus in this paper is the application of the method to a systematic investigation of the energetics of multiply charged metal-cluster anions (Sec. III). We showed that while singly charged anions are stable for all sizes (our calculated first-electron affinities are in good correspondence with experimentally measured ones), multiply charged negative ions are stable against spontaneous electron decay only above certain critical sizes, which we term borders of stability. Below a border of stability, multiply anionic clusters are metastable against autodetachment via electron tunneling through a Coulombic barrier. Lifetimes for such electron decay processes, which increase as one approaches the critical clusters size (i.e., the border of stability), were estimated by us for doubly negatively charged sodium clusters, using the WKB tunneling formula with self-interaction corrected (SIC) potentials. Since fission processes may provide competitive decay channels, the energetics of fragmentation of doubly charged sodium anions was discussed in Sec. III C.

Confrontation of our predictions with experiment would require measurements on mass-selected multiply negatively charged metal clusters. A method for generating such clusters may involve fragmentation (via heating or collisions) of large charged droplets produced by a liquid-metal source.

ACKNOWLEDGMENTS

This research was supported by a grant from the U.S. Department of Energy (Grant No. AG05-86ER45234).

[1] See articles in (a) *Elemental and Molecular Clusters*, edited by G. Benedek and M. Pacchioni (Springer, Berlin, 1988); (b) *Physics and Chemistry of Small Clusters*, edited by P. Jena, S. N. Khanna, and B. K. Rao (Plenum, New York, 1987); (c) *Physics and Chemistry of Finite Systems: From Clusters to Crystals*, edited by P. Jena, S. N. Khanna, and B. K. Rao (Kluwer, Dordrecht, 1992).

[2] W. A. de Heer, W. D. Knight, M. Y. Chou, and M. L. Cohen, in Solid State Physics, edited by H. Ehrenreich, F. Seitz, and D. Turnbull (Academic, New York, 1987), Vol. 40, p. 93.

[3] Fifth International Symposium on Small Particles and Inorganic Clusters, Konstanz, 1990 [Z. Phys. D **19** (1991); **20** (1991)].

[4] H. Nishioka, K. Hansen, and B. R. Mottelson, Phys. Rev. B **42**, 9377 (1990); J. Pedersen, S. Bjørnholm, J. Borggreen, K. Hansen, T. P. Martin, and H. D. Rasmussen, Nature **353**, 733 (1991); T. P. Martin, S. Bjørnholm, J. Borggreen, C. Bréchignac, Ph. Cahuzac, K. Hansen, and J. Pedersen, Chem. Phys. Lett. **186**, 53 (1991); T. P. Martin, T. Bergmann, H. Göhlich, and T. Lange, in *Cluster Models for Surface and Bulk Phenomena*, edited by G. Pacchioni *et al.* (Plenum, New York, 1992), p. 3; J. L. Persson, R. L. Whetten, H.-P. Cheng, and R. S. Berry, Chem. Phys. Lett. **186**, 215 (1991).

[5] W. A. de Heer, K. Selby, V. Kresin, J. Masui, M. Vollmer, A. Châtelain, and W. D. Knight, Phys. Rev. Lett. **59**, 1805 (1987); K. Selby, V. Kresin, J. Masui, M. Vollmer, W. A. de Heer, A. Scheidemann, and W. D. Knight, Phys. Rev. B **43**, 4565 (1991).

[6] W. Ekardt, Phys. Rev. B **31**, 6360 (1985).

[7] C. Yannouleas, R. A. Broglia, M. Brack, and P. F. Bortignon, Phys. Rev. Lett. **63**, 255 (1989).

[8] R. N. Barnett, U. Landman, and G. Rajagopal, Phys. Rev. Lett. **67**, 3058 (1991); see also R. N. Barnett and U. Landman, *ibid.* **69**, 1472 (1992); R. N. Barnett, U. Landman, A. Nitzan, and G. Rajagopal, J. Chem. Phys. **94**, 608 (1991).

[9] C. Bréchignac, Ph. Cahuzac, F. Carlier, and M. de Frutos, Phys. Rev. Lett. **64**, 2893 (1990); C. Bréchignac, Ph. Cahuzac, F. Carlier, J. Leygnier, and A. Sarfati, Phys. Rev. B **44**, 11 386 (1991).

[10] W. A. Saunders, Phys. Rev. Lett. **64**, 3046 (1990); **66**, 840 (1991).

[11] M. P. Iñiguez, J. A. Alonso, M. A. Aller, and L. C. Balbás, Phys. Rev. B **34**, 2152 (1986).

[12] Å. Bohr and B. R. Mottelson, *Nuclear Structure* (Benjamin, Reading, MA, 1975), Vol. II.

[13] M. A. Preston and R. K. Bhaduri, *Structure of the Nucleus* (Addison-Wesley, London, 1975).

[14] G. F. Bertsch and D. Tománek, Phys. Rev. B **40**, 2749 (1989).

[15] M. Nakamura, Y. Ishii, A. Tamura, and S. Sugano, Phys. Rev. A **42**, 2267 (1990).

[16] See also articles in (a) *Nuclear Physics Concepts in Atomic Cluster Physics*, edited by R. Schmidt *et al.* (Springer, Berlin, 1992); (b) *Clustering Phenomena in Atoms and Nuclei*, edited by M. Brenner *et al.* (Springer, Berlin, 1992).

[17] W. Ekardt and Z. Penzar, Phys. Rev. B **38**, 4273 (1988).

[18] Z. Penzar and W. Ekardt, Z. Phys. D **17**, 69 (1990).

[19] W. Ekardt, Phys. Rev. B **29**, 1558 (1984).

[20] D. E. Beck, Solid State Commun. **49**, 381 (1984).
[21] V. Bonačić-Koutecký, P. Fantucci, and J. Koutecký, Chem. Rev. **91**, 1035 (1991); J. Chem. Phys. **93**, 3802 (1990).
[22] U. Röthlisberger and W. Andreoni, J. Chem. Phys. **94**, 8129 (1991).
[23] C. F. von Weizsäcker, Z. Phys. **96**, 431 (1935).
[24] H. A. Bethe and R. F. Bacher, Rev. Mod. Phys. **8**, 82 (1936).
[25] See, in particular, *Structure of the Nucleus* (Ref. 13), pp. 202*ff*.
[26] W. D. Myers and W. J. Swiatecki, Nucl. Phys. **81**, 1 (1966).
[27] V. M. Strutinsky, Nucl. Phys. **A95**, 420 (1967).
[28] V. M. Strutinsky, Nucl. Phys. **A122**, 1 (1968).
[29] M. Brack, J. Damgård, A. S. Jensen, H. C. Pauli, V. M. Strutinsky, and C. Y. Wong, Rev. Mod. Phys. **44**, 320 (1972).
[30] See, in particular, *Nuclear Structure* (Ref. 12), pp. 598*ff*.
[31] M. Brack and P. Quentin, Nucl. Phys. **A361**, 35 (1981).
[32] C. Guet and M. Brack, Z. Phys. A **297**, 247 (1980).
[33] D. R. Snider and R. S. Sorbello, Solid State Commun. **47**, 845 (1983).
[34] Ll. Serra, F. Garcías, M. Barranco, J. Navarro, L. C. Balbás, and A. Mañanes, Phys. Rev. B **39**, 8247 (1989).
[35] M. Brack, Phys. Rev. B **39**, 3533 (1989).
[36] M. Membrado, A. F. Pacheco, and J. Sañudo, Phys. Rev. B **41**, 5643 (1990).
[37] E. Engel and J. P. Perdew, Phys. Rev. B **43**, 1331 (1991).
[38] M. Seidl, K.-H. Meiwes-Broer, and M. Brack, J. Chem. Phys. **95**, 1295 (1991).
[39] For an ETF study of the asymptotic behavior of the first ionization potential and the first electron affinity, cf. Refs. 37 and 38. For an ETF study of the asymptotic behavior of the position of the plasmon, cf. Refs. 34 and 35.
[40] The ETF approach has also been used to study fission barriers above the threshold where the fissility equals unity. In this repect, the importance of the missing shell corrections has been stressed [J. M. López, J. A. Alonso, F. Garcias, and M. Barranco, Ann. Phys. (Leipzig) **1**, 270 (1992)].
[41] C. Yannouleas and R. A. Broglia, Phys. Rev. A **44**, 5793 (1991); Europhys. Lett. **15**, 843 (1991); C. Yannouleas, P. Jena, and S. N. Khanna, Phys. Rev. B **46**, 9751 (1992).
[42] C. Yannouleas, Chem. Phys. Lett. **193**, 587 (1992).
[43] C. Yannouleas and R. A. Broglia, Ann. Phys. (N.Y.) **217**, 105 (1992); C. Yannouleas, E. Vigezzi, and R. A. Broglia, Phys. Rev. B **47**, 9849 (1993).
[44] W. Kohn and L. J. Sham, Phys. Rev. **140**, A1133 (1965).
[45] W. de Heer, Rev. Mod. Phys. **65**, 611 (1993).
[46] V. V. Kresin, Phys. Rep. **220**, 1 (1992).
[47] D. E. Beck, Phys. Rev. B **43**, 7301 (1991).
[48] J. Harris, Phys. Rev. B **31**, 1770 (1985).
[49] M. W. Finnis, J. Phys. Condens. Matter **2**, 331 (1990).
[50] H. M. Polatoglou and M. Methfessel, Phys. Rev. B **37**, 10 403 (1988).
[51] W. M. C. Foulkes and R. Haydock, Phys. Rev. B **39**, 12 520 (1989).
[52] C. Yannouleas and U. Landman (unpublished).
[53] T. H. R. Skyrme, Philos. Mag. **1**, 1043 (1956); Nucl. Phys. **9**, 615 (1959).
[54] M. Brack, in *Density Functional Methods in Physics*, edited by R. M. Dreizler and J. da Providencia (Plenum, New York, 1985), p. 331 (see, in particular, pp. 334*ff*).
[55] L.H. Thomas, Proc. Cambridge Philos. Soc. **23**, 542 (1926); E. Fermi, Z. Phys. **48**, 73 (1928).
[56] C. H. Hodges, Can. J. Phys. **51**, 1428 (1973).
[57] E. P. Wigner, Phys. Rev. **40**, 749 (1932); J. G. Kirkwood, Phys. Rev. **44**, 31 (1933).
[58] O. Gunnarsson and B. I. Lundqvist, Phys. Rev. B **13**, 4274 (1976).
[59] E. Zaremba, J. Phys. Condens. Matter **2**, 2479 (1990).
[60] The choice of the ETF energy functional as a vehicle for optimization of the input density is a rather natural one. Indeed, in several attempts (such as the integral formulation of density-functional theory [W. Yang, Phys. Rev. A **38**, 5494 (1988)] or through the use of generalized nonlocal kinetic-energy functionals [L.-W. Wang and M. P. Teter, Phys. Rev. B **45**, 13 196 (1992)]) to construct theories based on the Hohenberg-Kohn density-functional theorem [P. Hohenberg and W. Kohn, Phys. Rev. **136**, B684 (1964)] directly, that is without the use of orbitals, the ETF functional (see Wang and Teter, above) (with the kinetic functional expanded in density gradients) or the TF density (see Yang, above) appear as a limiting case or lowest level of approximation, respectively.
[61] C. Coulomb, *Mémoires de l' Académie* (1786), pp. 67*ff*; *ibid.* (1787), p. 452; M. Faraday, *Experimental Research in Electricity (1839)* (Dover, New York, 1965), Vol. I, pp. 360*ff*.
[62] For a study of highly charged *cationic* metal clusters, see T. P. Martin, U. Näher, H. Göhlich, and T. Lange, Chem. Phys. Lett. **196**, 113 (1992); U. Näher, H. Göhlich, T. Lange, and T. P. Martin, Phys. Rev. Lett. **68**, 3416 (1992).
[63] J. G. Eaton *et al.*, in *Nuclear Physics Concepts in Atomic Clusters* [Ref. 16(a)], p. 291.
[64] C. L. Pettiette *et al.*, J. Chem. Phys. **88**, 5377 (1988).
[65] G. Ganteför, M. Gausa, K.-H. Meiwes-Broer, and H. O. Lutz, J. Chem. Soc. Faraday Trans. **86**, 2483 (1990).
[66] G. Ganteför, K.-H. Meiwes-Broer, and H. O. Lutz, Phys. Rev. A **37**, 2716 (1988).
[67] J. M. Pacheco and W. Ekardt, Z. Phys. D **24**, 65 (1992).
[68] (a) For experimental studies of the first-electron affinity, cf. Refs. 63–66. For theoretical studies of the optical response of singly charged anions, cf. Refs. 42 and 67. (b) For some previous theoretical considerations of multiply charged anions, see A. Rubio *et al.*, Physica B **167**, 19 (1990); C. Yannouleas and U. Landman, Chem. Phys. Lett. **210**, 437 (1993).
[69] J. P. Perdew and A. Zunger, Phys. Rev. B **23**, 5048 (1981).
[70] L. C. Balbás, A. Rubio, and J. A. Alonso, Chem. Phys. **120**, 239 (1988).
[71] D. M. Wood, Phys. Rev. Lett. **46**, 749 (1981).
[72] M. P. J. van Staveren, H. B. Brom, L. J. de Jongh, and Y. Ishii, Phys. Rev. B **35**, 7749 (1987).
[73] J. P. Perdew and Y. Wang, Phys. Rev. B **38**, 12 228 (1988).
[74] Ph. J. Siemens and A. S. Jensen, *Elements of Nuclei* (Addison-Wesley, New York, 1987).
[75] We emphasize that while the effective potentials are significantly different when SIC is used, other quantities, such as the total energy, IP's, and EA's are only slightly altered by SIC as shown in Ref. 69 and by our own calculations.
[76] S. Hofmann, *Proton Radioactivity* in *Particle Emission from Nuclei*, edited by D.N. Poenaru and M.S. Ivascu (CRC, Boca Raton, FL, 1989), Vol. II, p. 25.
[77] A complete account of the application of the shell-correction method to triaxially deformed jellium droplets will be given in a forthcoming publication (Ref. 52).
[78] C. Bréchignac, Ph. Cahuzac, F. Carlier, and J. Leygnier, Phys. Rev. Lett. **63**, 1368 (1989).